https://doi.org/10.5194/egusphere-2026-1077
Preprint. Discussion started: 5 May 2026

Long-term land-atmosphere carbon monoxide exchange from a tall tower in a rural Central European region

László Haszpra[1,2], Zoltán Barcza[3,4], Anikó Kern[5,6], Natascha Kljun[7,8]

[1]HUN-REN Institute for Nuclear Research, H-4026 Debrecen, Hungary
[2]HUN-REN Institute of Earth Physics and Space Science, H-9400 Sopron, Hungary
[3]ELTE Eötvös Loránd University, Department of Meteorology, H-1117 Budapest, Hungary
[4]Global Change Research Institute, Czech Academy of Sciences, 603 00 Brno, Czech Republic
[5]Institute of Geography and Earth Sciences, ELTE Eötvös Loránd University, H-1117, Budapest, Hungary
[6]Institute for Electrophysics/SpaceLab, Obuda University, H-1034 Budapest, Hungary
[7]Centre for Environmental and Climate Science, Lund University, 223 62 Lund, Sweden
[8]Department of Earth and Environmental Sciences, Lund University, 223 62 Lund, Sweden

Correspondence to: László Haszpra (haszpra.laszlo@atomki.hu)

Abstract. Carbon monoxide (CO) is a crucial atmospheric trace gas, significantly influencing the atmosphere's oxidative capacity and indirectly affecting climate. However, the net land-atmosphere exchange of CO remains highly uncertain due to the scarcity of long-term monitoring. This study presents and analyses a 10-year-long CO flux data series from a tall-tower eddy covariance (EC) system operated in a rural Central European region. The measured fluxes were evaluated separately for cases when the flux footprint of the measurement covered almost exclusively quasi-natural areas (arable land, forests), and for cases when the footprint of the measurement covered populated areas (villages, roads). The vegetation-dominated sector (agricultural fields and forests) acted as a weak net CO source from April to September with an average emission of 0.58 nmol m^{-2} s^{-1} (monthly range 0.31–0.91 nmol m^{-2} s^{-1}), with the highest value occurring in July. The diurnal peaks of the median hourly emissions can be observed around noon, and they range from 1.59 to 2.66 nmol m^{-2} s^{-1}. The nighttime (20-04 h LST) hourly median values range from -1.01 to +1.17 nmol m^{-2} s^{-1}. Their deviations from zero are not statistically significant at a $p<0.05$ probability level. Solar radiation was identified as the primary driver of CO exchange. The measured emissions from the populated areas significantly exceed the activity-based estimations, presumably due to the underestimation of the emissions from residential heating. This study also presents the advantages and challenges of tall-tower EC flux measurements.

1 Introduction

For a long time, carbon monoxide (CO) was primarily considered a dangerous, toxic component of urban and indoor air pollution (Horner, 2000). With the introduction of three-way catalytic converters in gasoline-powered vehicles and advances in combustion technologies, carbon monoxide pollution has become less of a problem in cities, at least in the more developed parts of the world (Hedelius et al., 2021). However, carbon monoxide is also an important trace component of the

https://doi.org/10.5194/egusphere-2026-1077
Preprint. Discussion started: 5 May 2026

global atmosphere, playing a significant role in atmospheric chemical processes, governing its oxidative capacity, and through these, indirectly influencing the atmospheric greenhouse effect and climate change (Szopa et al., 2023).

Carbon monoxide is oxidized by the hydroxyl radical (OH). The product of this chemical reaction is carbon dioxide (CO_2), which is the second most important greenhouse gas in the atmosphere after water vapor (Schmidt et al., 2010). The oxidation of carbon monoxide by OH is a concurrent chemical reaction with the oxidation of methane by OH, which is the dominant sink of methane in the troposphere. One of the reaction products is carbon monoxide itself (Gaubert et al., 2017). The reaction of OH with carbon monoxide consumes about 40 % of OH radicals (Lelieveld et al., 2016; Zhao et al., 2020). Any change in the atmospheric carbon monoxide concentration influences the lifetime of methane, the third most important greenhouse gas after water vapor and carbon dioxide, and thus, CO could be considered an indirect greenhouse gas. The oxidation of carbon monoxide by OH also results in hydroperoxyl radicals. Hydroperoxyl radical is one of the key components of ozone formation in the troposphere (Crutzen et al., 1999). In addition to being a greenhouse gas, ozone is also a phytotoxic substance of environmental concern. All this underscores the importance of research focusing on the sources, sinks, and processes of atmospheric carbon monoxide.

Almost half of the carbon monoxide in the atmosphere is derived from the oxidation of methane and other volatile organic compounds. One quarter comes from direct anthropogenic sources, and a roughly similar amount from biomass burning, which has large interannual variability. The source inventory is completed by a minor (~7 %) biogenic and a practically negligible (<1 %) oceanic release (Zheng et al., 2019). In the recent compilation of Zheng et al. (2019), oxidation by OH is the only globally notable sink of carbon monoxide. Other authors (e.g., Khalil et al., 1999; Pihlatie et al., 2016; Liu et al., 2018; and references from therein) suppose that soils are globally a small but not negligible sink of CO due to microbial oxidation processes (Ragsdale, 2004; King and Weber, 2007). Duncan et al. (2007) list several inversion studies, a part of which attributes up to 10 % of the global CO-sink to the soil, while the others did not indicate a net soil sink. Their own model supposes that biogenic emissions are roughly balanced with the amount consumed by soils, and that these emissions exert no significant net influence on the global CO budget.

The scarce availability of in-situ CO flux data comes from relatively few, mostly short-term measurements performed at a limited spatial context (using e.g. chambers and short (<5 m) eddy covariance (EC) towers), which cannot represent the wide variety of ecosystems, soil types, and climate conditions, and regional scale fluxes. The CO-consuming microbial activity may depend on the organic fraction of the soil, porosity, temperature, water content, etc., while the production rate of carbon monoxide via thermal- or photodegradation of the living or dead organic matter may depend on plant species (Bruhn et al., 2013). Bruhl et al. (2013) conducted a 2-month survey over a grassland in Denmark using UV-transparent Plexiglas chambers and found that the grassland was a net sink. Constant et al. (2008) came to the same conclusion after one year of CO-flux measurement over a grassland in Canada using the vertical gradient method at a 3 m-tall tower. However, the 20-month-long survey of Cowan et al. (2018) over a grazed grassland in Scotland indicated net emission from the soil-vegetation system, not supporting the net soil sink hypothesis. Lassonen et al. (2025) performed a 2-year-long measurement series over an Arctic peatland in Sweden and concluded that part of the peatland could act as either a net source or sink,

https://doi.org/10.5194/egusphere-2026-1077
Preprint. Discussion started: 5 May 2026

depending on soil moisture levels. However, the area as a whole, as represented by the measurements, acted as a net CO source. Lassonen (2021) studied three different ecological systems in Finland (6–23 months) and one in Kenya (1 month), and found all to be net CO sources, as the soil uptake was overcompensated by the mainly radiation-driven emission. The 22-month-long measurement by Murphy et al. (2023) over a fertilized and grazed grassland in Ireland did not show net CO uptake by soil either. Pihlatie et al. (2016) reported on a single season (from snowmelt to snowfall) of CO-flux measurements over an area cultivated with a perennial reed canary grassland in Finland. They found a seasonally variable net flux direction. The represented area was a net source from mid-April to mid-June, and a net sink from mid-June to November. Integration of the fluxes over the 7 months of the measurements indicated a weak net soil uptake. Pihlatie et al. (2016) also list several earlier CO-flux monitoring projects from different parts of the world, which indicate a mixture of positive and negative CO fluxes between the surface and the atmosphere. Sun et al. (2018) also recorded net soil uptake during a project covering a late growing season (July–November) in a Scots pine forest in Finland. Based on two short measurement campaigns, van Asperen et al. (2024) concluded that soil sources dominate over soil sinks in tropical rainforests in Brazil.

The general conclusion is that the net biogenic CO exchange between the land surface (soil + vegetation) and the atmosphere is highly uncertain due to the limited number of measurement projects and the rather short (from a few days to about 2 years) monitoring periods. Although the biogenic surface-atmosphere exchange is not the major contributor to the atmospheric CO budget, due to the wide-ranging effects of carbon monoxide in the global environment, it is worth clarifying this contribution.

Most of the historic measurements applied the so-called chamber method, which involved open or closed, opaque or transparent chambers of various sizes. This labor-intensive method cannot cope with the heterogeneity of the soil; moreover, its spatial representativeness is rather limited. The micrometeorological methods suitable for continuous monitoring of CO-fluxes only appeared about a decade ago (Blomquist et al., 2012; van Asperen et al., 2015; Pihlatie et al., 2016). To date, only a few, mostly short-term projects lasting from a few days to a maximum of two years, have been published (Blomquist et al., 2012; van Asperen et al., 2015; Pihlatie et al., 2016; Cowan et al., 2018; Murphy et al., 2023; Laasonen et al., 2025). These studies used short, 2–4 m tall towers and focused on specific ecological systems. The use of taller towers comes with significant benefits, but also poses challenges (see e.g. Berger et al., 2001; Davis et al., 2003; Desai et al., 2015; Chi et al., 2019; Herig Coimbra et al., 2024; Hilland et al., 2025; and several other publications). Tall-tower measurements can provide landscape-scale surface-atmosphere exchange values over heterogeneous regions of up to 100 km^2 or more, depending on the height of the tower (Kljun et al., 2002; Kljun et al., 2004; Barcza et al., 2009; Desai et al., 2015; Chi et al., 2019; Barcza et al., 2020), and these values can be more robustly upscaled than the data from specific ecosystems. At the same time, the flux measurement on a tall tower may become decoupled from the surface during low-level temperature inversions, and temporary accumulation of material in the atmospheric layer below the measurement level („storage”) may also cause methodological challenges (Haszpra et al., 2005).

https://doi.org/10.5194/egusphere-2026-1077
Preprint. Discussion started: 5 May 2026

This study focuses on a tall tower site in western Hungary. Here, atmospheric carbon monoxide concentration monitoring started already in 2015. The high-frequency data acquisition and the availability of a co-located EC system for CO_2 ecosystem exchange measurements (Barcza et al., 2020) raised the idea that these measurements could also be used to determine the flux of carbon monoxide between the surface and the atmosphere. We are aware of only a few recent short-term (<1 year) attempts to measure CO-flux on tall tower (Helfter et al., 2016; Coimbra et al., 2024; Hilland et al., 2025). These measurements were performed in urban or semi-urban environments. As the original purpose of the measurements was the long-term monitoring of the concentration trends, local auxiliary measurements for the interpretation of the flux measurements are limited. Despite these challenges, this study presents the first long-term, tall-tower-based, regionally representative CO flux data series for a rural environment for the 2015–2025 period.

2 Measurements and methods

2.1 Site location and instrumentation

The Hegyhátsál tall-tower greenhouse gas monitoring station is located in a rural environment in western Hungary (46.956°N, 16.652°E, 248 m asl). It was established in 1993 and provides data for the Global Atmosphere Watch of the World Meteorological Organization (WIGOS ID: 0-348-4-16307) and weekly air samples are taken for NOAA's Global Cooperative Flask Air Sampling Network (NOAA station ID: HUN). Since 2024, the site has also been operating as an ICOS Class 2 atmospheric site. The station is a 117 m-tall TV/radio transmitter tower operated by Antenna Hungária Corp., equipped with meteorological sensors and air intake tubes at different elevations (10 m, 48 m (50 m from 2022), 82 m, 96 m, 115 m above the ground).

The station is located in a fairly flat region, in the vicinity of a small village called Hegyhátsál. During the 10 years of this study (July 2015 – June 2025), the population of the settlement, accommodating no industrial or commercial activities, gradually decreased from 160 to 141 people (Hungarian Central Statistical Office, 2025). The village, a potential anthropogenic carbon monoxide source, is located in the northwest sector of the station, at a distance of 400–1200 m, while the prevailing wind direction is perpendicular to this direction. Apart from the village, the tower is surrounded by a regionally typical mixture of agricultural fields (dominantly corn, winter wheat, and rape in crop rotation with small plots of other cultivars) and forest patches. For the identification of the land cover types, the National Ecosystem Base Map of Hungary (NÖSZTÉP) (Tanács et al., 2021) was used. This dataset classifies 56 land cover type categories and provides land cover information with a spatial resolution of 20 m×20 m (Fig. 1). The soil type in the region is 'Lessivated brown forest soil' (Alfisol, according to the USDA system). The upper layer is generally 10–20 cm thick and has an organic matter content of 5–8 %.

https://doi.org/10.5194/egusphere-2026-1077
Preprint. Discussion started: 5 May 2026

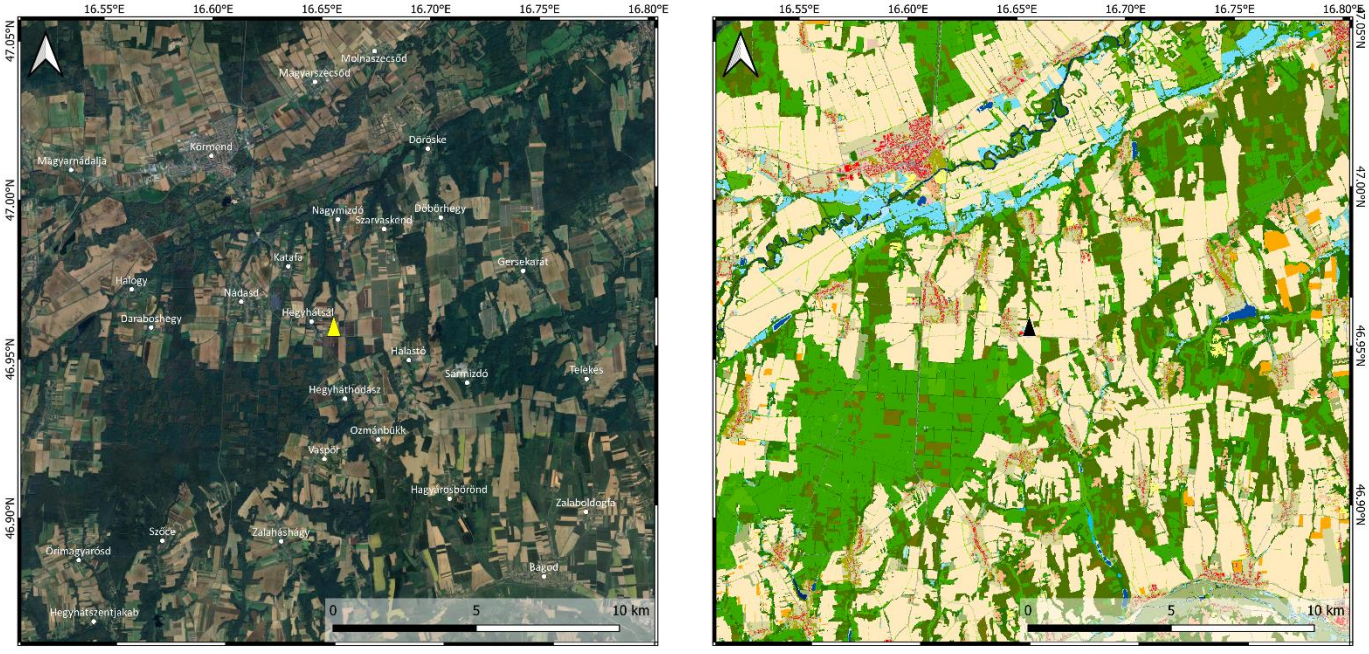

130

Figure 1: Google Earth satellite image (left – © Maxar Technologies/Google, 2025) and the NÖSZTÉP land cover map (right) of the region of the monitoring site (colors: shades of green – different types of forests and grasslands, yellow to pale orange – agricultural lands, bluish – wetlands, rivers, lakes, red/pink – buildings/urban areas, olive – green areas in urban environment; for detailed description see Tanács et al., 2021). Location of the tower is indicated by a yellow (left) and black (right) triangle.

135

The neighboring villages near Hegyhátsál are about 3 km away from the tower to the northwest (Katafa), west (Nádasd), and south (Hegyháthodász). The nearest settlement worth mentioning in the eastern sector is Gersekarát, located more than 7 km from the tower (Fig. 1). There is hardly any commercial or industrial activity in this predominantly agricultural region. The local roads connecting the small settlements carry little traffic (300–600 vehicle units per day). The only major road in the 140 region is the 2×1-lane trans-European E65 running northwest–southeast with 5200 vehicle units per day (Magyar Közút, 2025). Its closest point to the monitoring site is about 500 m to the southwest (Fig. 1).

Carbon monoxide concentration has been monitored using an Enhanced Performance fast-response N_2O/CO/H_2O analyzer (Model 913-0014, Los Gatos Research Ltd., San Jose, CA, U.S.A.) with fast-flow optional accessories, which records at 5 Hz frequency continuously since July 2015. The analyzer is located at ground level in an air-conditioned room of the 145 transmitter building. Air to be analyzed is taken from 82 m on the tower through an approximately 100 m-long 3/8" OD Synflex 1300 tube (Eaton Corporation Plc, Dublin, Ireland). The flow rate at about 3.5 L/min is maintained by a diaphragm vacuum pump (KNF Type N 880.3 AN.22E, Neuberger, Inc., Trenton, NJ, U.S.A.). The analyzer is regularly calibrated against four CO-in-natural air standards (48-513 nmol mol^{-1}) produced and certified by Max Planck Institute for Biogeochemistry, Jena, Germany, to meet the high accuracy requirements of the monitoring of the temporal variation in the

https://doi.org/10.5194/egusphere-2026-1077
Preprint. Discussion started: 5 May 2026

concentration (long-term trend, seasonal and daily variations, etc.) (WMO, 2024). The standards are traceable to the WMO CO X2014A scale. The drifts of the standards were linearly corrected between the recalibrations of the standards, and we continuously compared the measurement results with those obtained from NOAA flask air samples to detect any significant drift.

The platform at 82 m elevation also hosts an EC system for the long-term monitoring of surface-atmosphere CO_2 exchange, consisting of a GILL R3-50 research ultrasonic anemometer and a LI-COR Model LI-6262 CO_2/H_2O analyzer (LI-COR Inc., Lincoln, Nebraska, USA; Barcza et al., 2020). The temporal synchronization of the monitoring systems and the close mounting of the intake tube of the N_2O/CO analyzer to the ultrasonic anemometer (~50 cm) allow us to use the analyzer not only for concentration monitoring but also to estimate the surface-atmosphere carbon monoxide exchange. Considering the high elevation of the EC system above the ground (82 m), where the characteristic size of the eddies is larger than that at the elevation of the usual EC systems (typically a few meters above the ground), the 5 Hz sampling frequency and the 3.5 L/min flow rate are sufficient for reliable flux calculations.

2.2 Auxiliary data

The monitoring system was not originally designed for a carbon monoxide exchange study; therefore, only some CO-flux-relevant auxiliary measurements are available from the site.

Air temperature is measured at 10 m elevation above the ground (until November 2022: Vaisala Model HMP35D; from December 2022: Vaisala Model HMP155; Vaisala Oyj, Helsinki, Finland), matching the lowest measurement elevation of the vertical CO_2 concentration profile (Haszpra et al., 2001). A Model LI-190SZ (LI-COR Inc., Lincoln, Nebraska, USA) quantum sensor was available until March 2021, followed by an Apogee SQ-100X-SS sensor (Apogee Instruments, Inc., Logan, Utah, USA) from December 2022 for recording of the incoming photosynthetically active radiation (0.4–0.7 μm) at 2 m above the ground.

UV-radiation and soil water content (SWC) may also influence the carbon monoxide exchange between the surface (vegetation+soil) and the atmosphere (Bruhn et al., 2013; Murphy et al., 2023; Laasonen et al., 2025). These data (downward UV-radiation at the surface [0.20–0.44 μm], volumetric soil water content in layer 0–7 cm) were downloaded from the ERA5 reanalysis dataset of the European Centre for Medium-Range Weather Forecasts (Copernicus Climate Change Service, 2022) for the nearest two grid points to the monitoring station (47.0°N, 16.5°E; 47.0°N, 16.75°E), and were then averaged.

A disadvantage of tall-tower EC systems is that they may be decoupled from the surface by low-level inversions from time to time (Desai et al., 2015; Chi et al., 2019). In these situations, the EC systems cannot provide the actual surface–atmosphere flux data. To remove decoupled measurements in cases of low-level inversion, information on the height of the boundary layer was also derived from the ERA5 reanalysis dataset.

https://doi.org/10.5194/egusphere-2026-1077
Preprint. Discussion started: 5 May 2026

2.3 Flux calculation

The basic theory of the EC flux measurement technique is discussed in the scientific literature in detail (see e.g. Aubinet et al. (2012) for summary and review). The methodology applied for the calculation of the raw hourly turbulent flux of CO at our tall tower monitoring site is practically identical to that used for CO_2 flux calculation at this site and is described in detail in Barcza (2001) and Barcza et al. (2020).

The turbulent flux calculation starts with the determination of the lag time caused by the ~100 m long air intake tube. For each day, lag time estimation was done interactively by visualizing the lagged covariance data for predefined time windows. Angle-of-attack dependent calibration was applied to the raw sonic anemometer data (van der Molen et al., 2004). Three-dimensional wind vector rotation was applied to align the coordinate system with the prevailing streamlines (Lee, 1998). The hourly means of the turbulent fluxes were calculated taking into account the predetermined lag times. As the system calculates fluxes from dry air mole fractions of CO, the Webb-Pearman-Leuning correction (Webb et al., 1980) was not applied. As part of the postprocessing, spectral corrections were applied to account for flux losses caused by the fluctuation damping caused by the intake tube, lateral sensor separation, sensor line averaging, etc. (Moore, 1986; Massman, 1991).

An EC system measures the mass transport through a horizontal plane at its elevation above the ground, which is 82 m in our case. In situations of limited vertical mixing, the EC system may become decoupled from the surface, causing the measurements to fail to reflect the actual processes taking place at the surface. To avoid the unrepresentative values, we did not calculate fluxes for those hours when the boundary layer height was below 100 m. The layer below the EC system may become enriched (surface source) or depleted (surface sink) in the trace gas studied without recording. After the decoupling (i.e., during the breakup of the nighttime inversion after sunrise), the accumulated excess or deficiency in the surface layer appears in the measured flux (storage flux). Although the temporary decoupling may distort the measured diurnal variation, the daily total flux usually properly reflects the daily surface-atmosphere exchange (as there is no long-term accumulation or depletion below the measurement level). Unlike in the case of CO_2, we suppose that emitted CO is neither taken up nor reemitted during the time of decoupling, i.e., there should not be any distortion of the net exchange estimations. Due to the absence of vertical concentration profile measurements, we have to accept the aforementioned limitations and assumptions.

We expect that due to the heterogeneous landscape surrounding the tower, the different land cover sections (arable lands, forests, villages, etc.) may contribute significantly different fluxes to the measured signal. Hence, no outlier filtering was applied during the flux calculation.

2.4 Flux footprint calculation

The flux footprint function quantifies the relative contribution of each element of the upwind surface area to the measured flux as a probability density function. For the calculation of the source area (footprint) of the flux measurements, the two-dimensional Flux Footprint Prediction (FFP) model developed by Kljun et al. (2015) was applied. This model performed

https://doi.org/10.5194/egusphere-2026-1077
Preprint. Discussion started: 5 May 2026

amongst the best in a test against data from a tracer release experiment involving several footprint models (Heidbach et al., 2017).

The input parameters of the model are the measurement height above displacement height (z_m), the roughness length (z_0), the Obukhov length (L), the standard deviation of the lateral wind speed (σ_v), the friction velocity (u_*), and the height of the boundary layer (h). The wind direction is an optional input parameter, but it is needed here for the geographical localization of the source areas. Displacement height was considered to be negligible relative to the height of the measurements; thus, the observation height was used to approximate z_m. The listed parameters were either directly measured or could be calculated from the measurements. The boundary layer height was available from the ERA5 reanalysis dataset (see Section 2.2) for the region of the tower. The roughness length was assumed to be equal to 0.15 m based on an earlier study (Barcza et al., 2009).

In this study, the model was used with the following restrictions: $20z_0 < z_m < h_e$, $-15.5 \leq z_m/L$, and $u_* \geq 0.2$ m s^{-1}, where h_e is the height of the entrainment layer. h_e is typically around 0.8 h, (Holtslag and Nieuwstadt, 1986; Kljun et al., 2015).

An example footprint climatology of the station for the year 2020 is presented in Fig. 2. It demonstrates that the prevailing wind directions at the station are northeasterly and southwesterly, and that the footprints for these wind directions typically extend up to 10 km from the tower.

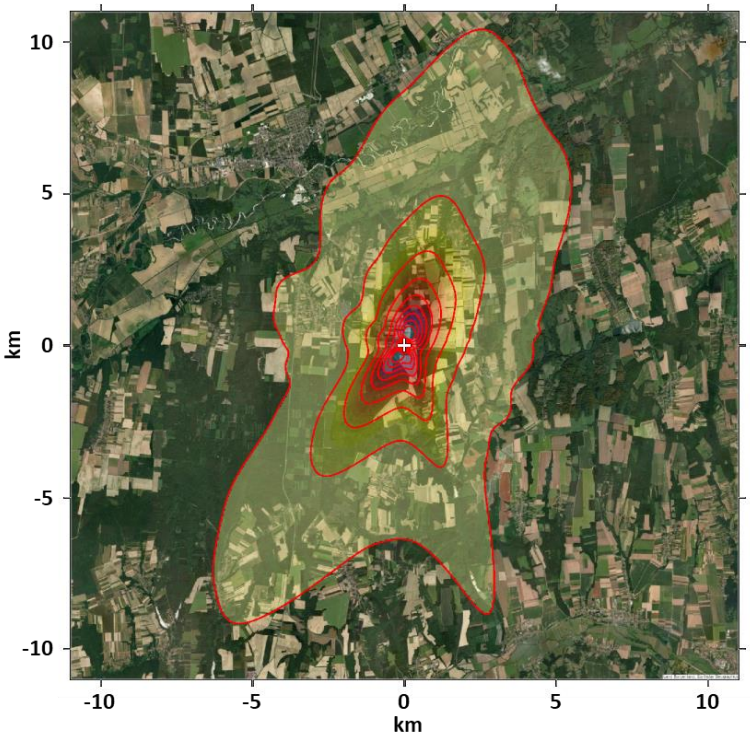

Figure 2: Flux footprint climatology of the monitoring site in 2020. For data selection, see Section 2.5. The footprint contour lines (red) show a 10 %–90 % contribution to the flux measurement in 10 % steps. The tower is at the origin (0,0) of the map, and indicated by a white + sign. Sources base map: ESRI | Powered by ESRI.

https://doi.org/10.5194/egusphere-2026-1077
Preprint. Discussion started: 5 May 2026

2.5 Data availability statistics

The measurements started on 1 July 2015, and the present study evaluates the data until 30 June 2025. The 10-year-long data series comprises 87,672 hourly values. During a total of 21,802 hours, predominantly summer nights and at any time of day in winter (see the boundary layer height statistics in Haszpra and Barcza (2010)), the boundary layer height was below 100 m. Due to the potential decoupling of the EC system from the surface, we rejected these data points for surface flux estimation. In the case of an additional 16,499 hours, fluxes could not be calculated for technical reasons. Finally, 14,068 hours did not satisfy the conditions for footprint calculations. In the absence of a solid theoretical basis, and also in order to avoid inclusion of modelled data, data gap filling was not applied.

Far-reaching flux footprints are increasingly uncertain and may cover distant anthropogenic sources, distorting the regional emission estimations. We selected only those footprints for which the integral of the footprint transfer function over a radius of 5 km from the tower was ≥0.8, i.e., the footprint contribution to the fluxes measured at the tower was ≥80 %. Altogether, we had to exclude 70.4 % of the hourly data; that is, 25,917 hourly data remained available for the actual study.

2.6 Flux map, and separation of populated and (quasi)natural areas

Using the filtered CO fluxes, footprint-weighted flux maps were calculated. In these maps, each grid cell contains the average of the fluxes measured at the tower weighted by the value of the footprint transfer function at the given grid cell. This approach only indicates the direction of the sources/sinks due to the so-called "blurring effect", and is not suitable on its own for determining the exact location of the sources/sinks (Rey-Sanchez et al., 2022).

In the case of most conventional eddy covariance towers, which are only a few meters tall, the heterogeneity of the footprint area is generally small. However, in the case of tall towers with an extensive footprint area, it can be significant. While tall towers are great for determining the average emissions of heterogeneous areas (Desai et al., 2015; Peltola et al., 2015; Chi et al., 2019) and allow more reliable upscaling of the results, attempts can also be made to separate fluxes from areas with different land cover types (Barcza et al., 2009; Helbig et al., 2017; Tuovinen et al., 2019; Hernandez Rodriguez et al., 2023; Tikkasalo et al., 2025). In this study, we use a simple method to determine the carbon monoxide flux of populated grid cells and (quasi)natural grid cells separately. A grid cell is considered „populated” if it belongs to one of the following NÖSZTÉP land use categories: buildings, roads, other paved or unpaved artificial surfaces, as well as green fields in an artificial environment. The term “(quasi)natural grid cell” refers to the categories of arable land, forest, grassland, and wetland, where the anthropogenic emissions are assumed to be minimal. Due to the relatively small amount of data, we did not attempt to separate the fluxes from agricultural fields and forests.

https://doi.org/10.5194/egusphere-2026-1077
Preprint. Discussion started: 5 May 2026

3 Results

3.1 Directional distribution of carbon monoxide flux

Figure 3 shows the footprint-weighted flux maps for the summer and winter months separately for the entire measurement period. The figure shows that the flux is higher from the direction of the village (west-northwest) than from the sector dominated by agricultural fields and forests. This result provides a solid basis for the separation of the populated (i.e. anthropogenic emission related) and dominantly natural areas with vegetation cover.

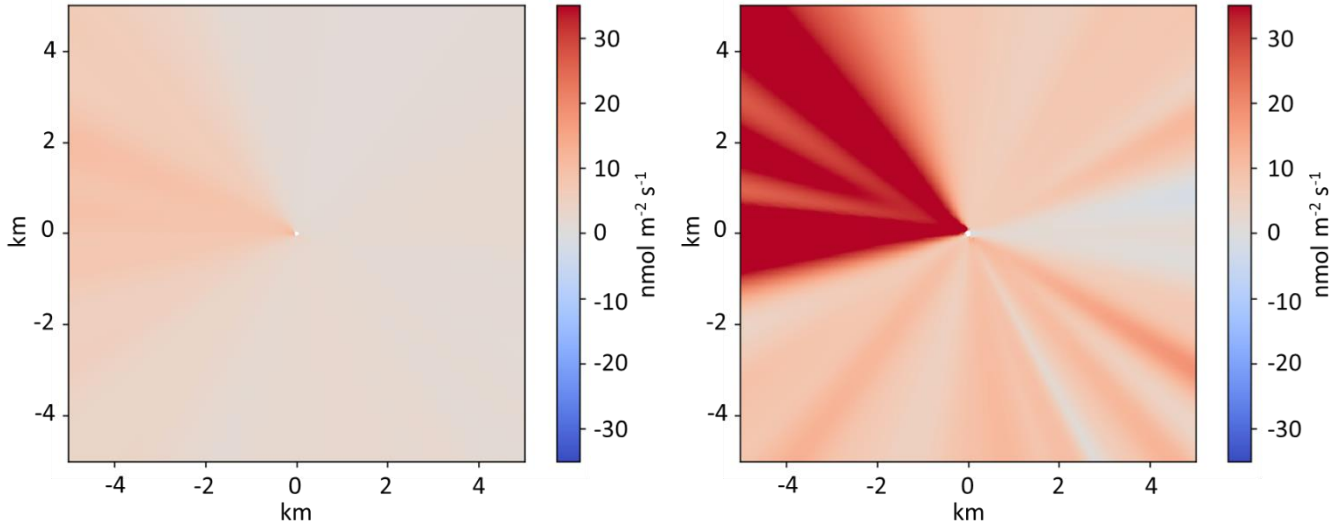

Figure 3: Footprint-weighted flux maps for the summer (Jun–Aug, 2015-2025, left) and winter months (Dec-Feb, 2015-2025, right). The maps are based on cases in which the footprint contribution over a radius of 5 km from the tower is at least 80 % to the measured fluxes. The tower is at the origin (0, 0).

3.2 Carbon monoxide emission from the populated areas

Based on the footprint selections described in Section 2.5 and source area separation presented in Section 2.6, the flux contribution from the populated area of the nearby small village of Hegyhátsál can be up to 42 %. High values are typical when the wind blows from the 275-290° sector. In the same sector but farther from the tower (2.5–3.5 km), there is a larger village called Nádasd (population: 1,300). In the case of far-reaching footprints in this direction, the flux contribution from this settlement may reach 14 %. Hegyháthodász, similar in population to Hegyhátsál, is located 1.8–2 km south of the tower. The flux contribution from this village may also reach 17 % during southerly winds. Neither of these settlements has notable industrial or commercial activities. Hence, carbon monoxide emissions should primarily originate from domestic activities, such as residential heating, which is typical in winter, and from the traffic year-round. Due to the absence of hot spots, it is assumed that anthropogenic emissions are uniformly distributed in the populated areas. Thus, the integrals of the footprint transfer function over these areas directly give their contributions to the measured flux.

https://doi.org/10.5194/egusphere-2026-1077
Preprint. Discussion started: 5 May 2026

The measured flux (f) is the sum of the flux from the populated areas (F) and that from the non-populated, (quasi)natural areas (f_{bg}). For the determination of the emissions from the populated areas, the following model was used:

$$F = (f - f_{bg}(1- \alpha))/\alpha \,, \qquad (1)$$

where α is the contribution of the populated grid cells. Assuming at least an order of magnitude difference between the fluxes from the populated areas and from the (quasi)natural areas ("background flux"), we used the initial guess of $f_{bg} = 0$ for the calculation. The emission density estimated this way for the populated grid cells will be used in the next section for a more realistic estimation of f_{bg}, which will then be used iteratively to refine the emission density of the populated cells.

If there are only a few populated grid cells, they are not necessarily representative of the populated areas in general. Therefore, the higher the α-value, the more robust the estimation. On the other hand, a higher α-value implies that less data are available for the calculations, which reduces the accuracy of the estimations. As a compromise, and to demonstrate the robustness of the estimation, the calculated median emissions for the populated areas are presented in Fig. 4 for the cases when the flux contribution from the populated grid cells is ≥20 %, ≥25 %, ≥30 %, and ≥35 %, respectively. As can be seen in the figure, the differences are minimal. The significant seasonal variation and the small amount of available data for each month prevent the estimation of the diurnal variation of the fluxes. For the same reason, we could not estimate the 2015-2025 trend either. In the following, the calculations are based on the 2015-2025 median value calculated for those cases when the flux contribution from the populated grid cells is ≥25 %.

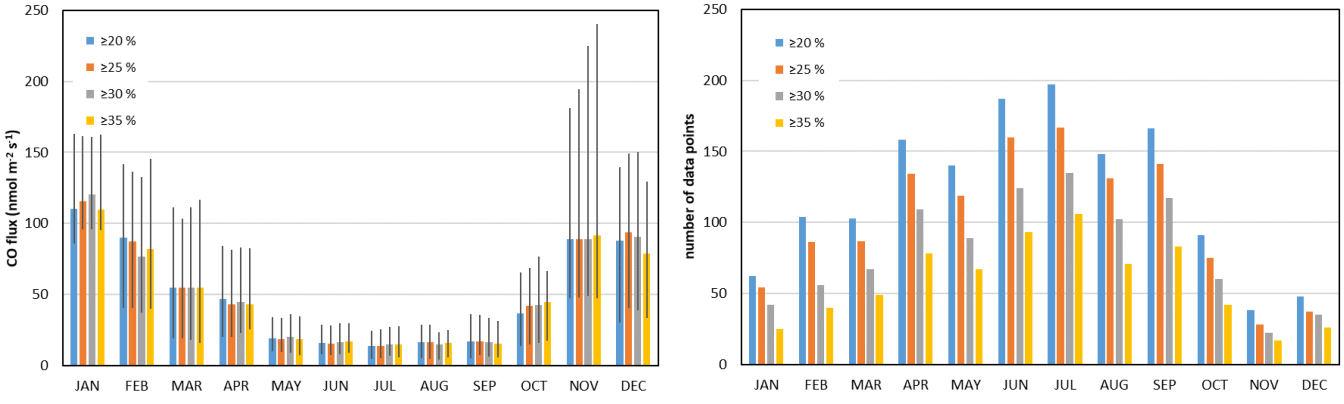

Figure 4: 2015-2025 monthly mean carbon monoxide fluxes from the populated areas (left panel) and the number of data available for the calculations (right panel). The flux values are calculated for ≥20 %, ≥25 %, ≥30 %, and ≥35 % flux contribution from the populated grid cells, assuming zero net flux from the (quasi)natural grid cells. The whiskers indicate the lower and upper quartiles. The right panel shows the decreasing data availability with the increasing flux contribution.

https://doi.org/10.5194/egusphere-2026-1077
Preprint. Discussion started: 5 May 2026

3.3 Carbon monoxide exchange of the vegetation-dominated landscape, and the refinement of the emissions from populated areas

For flux measurements at a height of 82 m in a densely populated Central European region, it is practically impossible to exclude roads and small agricultural buildings from the footprints of the measurements in any direction. For the determination of the carbon monoxide exchange of the vegetation-dominated, (quasi)natural landscape (agricultural fields, forests), we selected those hourly footprints for which ≥80 % of flux contribution came from within a 5 km radius of the tower (see also Section 2.5), and the flux contribution from the so-called populated grid cells did not exceed 2.5 %. The median contribution of the populated grid cells to the measured fluxes over the 12,347 selected hours was 1.74 %. The contribution of arable land to the measured flux varied between 11 % and 78 %, while the corresponding values for forested areas were 7 % and 68 %, depending on the location and extent of the actual footprint. This sector characteristically corresponds to the wind directions of 350–150° and 190–230° (see Fig. 3).

Even if the populated grid cells cover only a small portion of the footprint area, their high emission density may still significantly influence the measured fluxes. To reduce this influence, an iterative process was applied. At any time, the measured flux is the combination of the flux from the populated grid cells and that from the cells of agricultural fields or forests. Using an estimated emission value from the populated grid cells (see Section 3.2), and rearranging equation (1), we can express the CO exchange of the (quasi)natural grid cells (f_{bg}):

$$f_{bg} = (f - \alpha F)/(1 - \alpha) \qquad (2)$$

For the populated grid cells, the emission density (F) calculated in the previous section for ≥25 % footprint flux contribution (cf. Fig. 4) was assumed for each month. Substituting the calculated f_{bg} value into equation (1) yields a modified F value, which is then used in equation (2) again. The results indicated that this iterative procedure quickly converges. Even after the 2nd round, the calculated fluxes hardly change. Figure 5 shows the changes in the calculated emissions from the populated grid cells in each month and in each iteration step. While the change in F was up to 13 % in the 1st iteration step, it was less than 0.4 % in the 2nd step, and less than 0.02 % in the 3rd step. The results obtained in the 3rd iteration step are considered the actual emission densities of the populated grid cells, and are discussed further in Section 4.1.

https://doi.org/10.5194/egusphere-2026-1077
Preprint. Discussion started: 5 May 2026

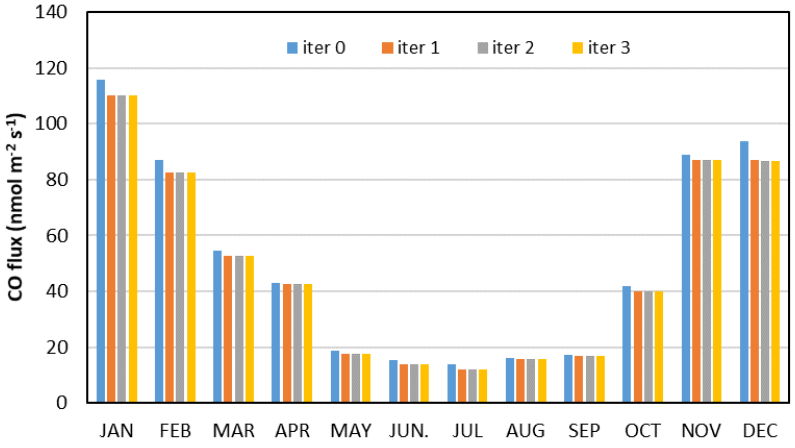

Figure 5: Iterative approximation of the emission density from the populated areas using the method described in the text. Iteration 0 (iter 0) represents the uncorrected data calculated in Section 3.2 (see Fig. 4). The flux values are calculated for the cases when the contribution of the populated grid cells to the measured fluxes at the tower is at least 25 %.

Figure 6 shows the mean diurnal variation of net CO exchange for each month based on the converged data. Lacking an objective criterion for defining a data point as „extreme", outlier removal was not applied during the quality control of the data. However, outliers (whether extreme or not) may distort the averages; therefore, Fig. 6 shows the median value for each hour of each month. The symbols in the figures indicate the confidence level of the deviations of the values from zero as determined by the Wilcoxon hypothesis test. It should be noted that significantly fewer data were available for nighttime hours than for daytime hours (especially in summer), affecting the confidence limits. As mentioned earlier, the limited data availability meant that the diurnal variation of the emission of the populated grid cells could not be derived. Therefore, the monthly average emissions were used to derive the natural CO flux, which can affect the estimated diurnal variation of the latter. Presumably, both anthropogenic and natural CO emissions are lower during night than during day; therefore, the limitation in the correction algorithm does not significantly alter the diurnal shape of the CO exchange over the arable land/forests.

https://doi.org/10.5194/egusphere-2026-1077
Preprint. Discussion started: 5 May 2026

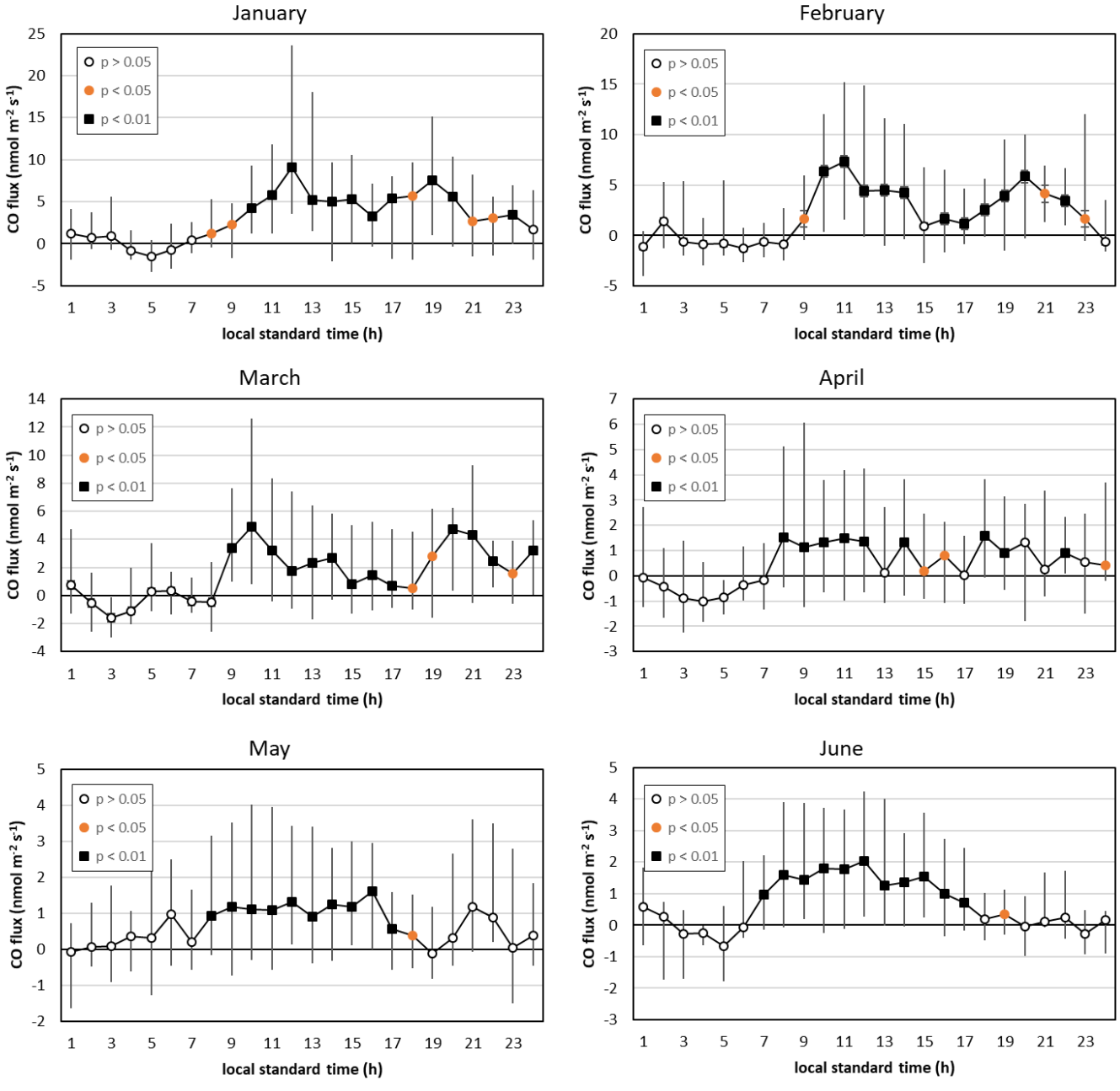

340

https://doi.org/10.5194/egusphere-2026-1077
Preprint. Discussion started: 5 May 2026

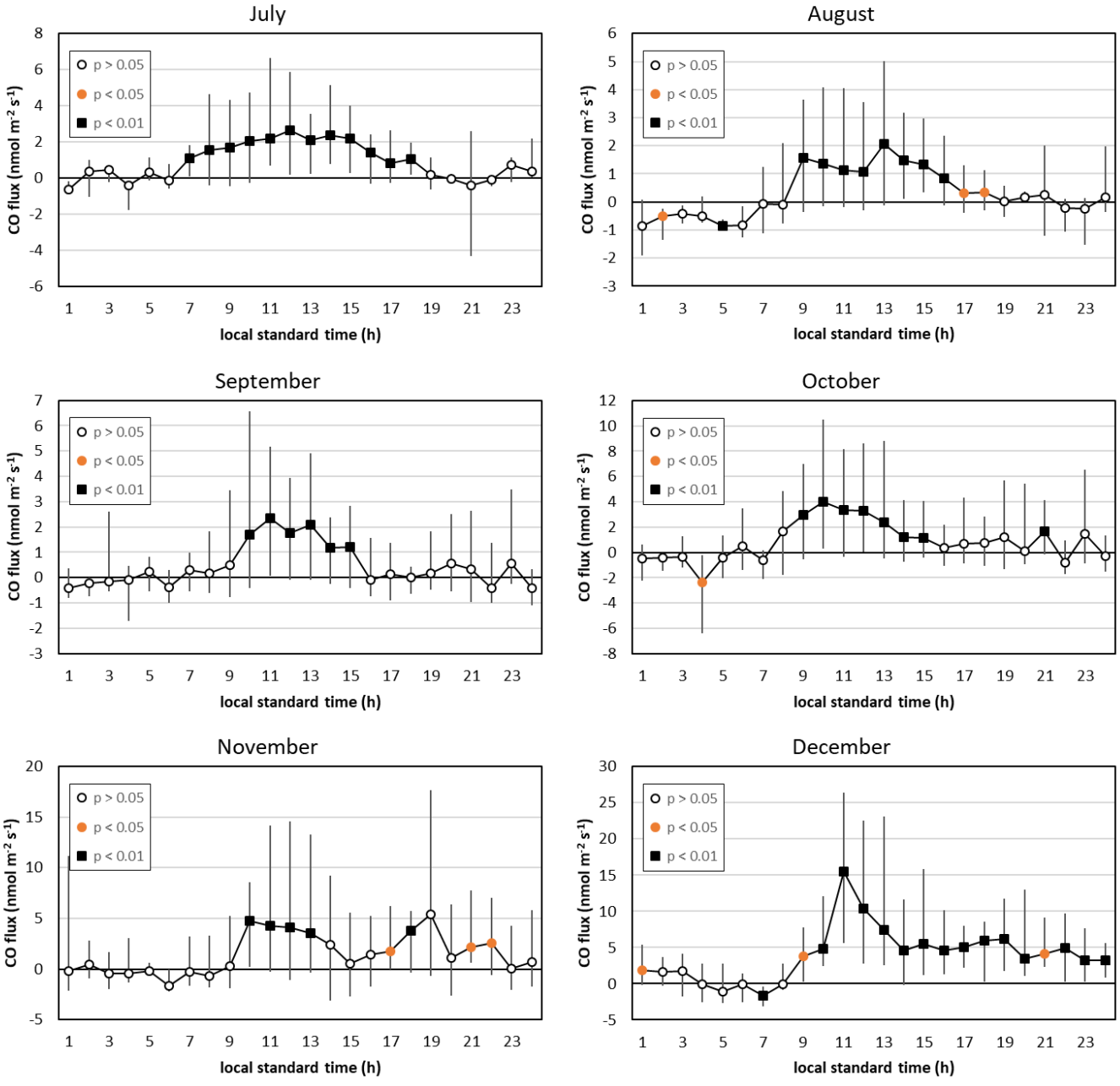

Figure 6: Mean diurnal variation of net CO exchange in the (quasi)natural grid cells (2015-2025). Whiskers indicate the lower and upper quartiles, while the symbols give the probability level of the deviation of the median from zero. Note the different y-axes.

345

https://doi.org/10.5194/egusphere-2026-1077
Preprint. Discussion started: 5 May 2026

The mean daily flux for each month can be calculated from the monthly mean diurnal variations of the hourly median fluxes (Fig. 7). Fluxes from the (quasi)natural grid cells are only a few percent of those from the populated grid cells (Fig. 5). The winter maximum in the net exchange over vegetated landscape cannot be explained by natural processes alone. It is hypothesized that our simple method cannot completely filter out the anthropogenic emissions. This question will be discussed further in Section 4.2.

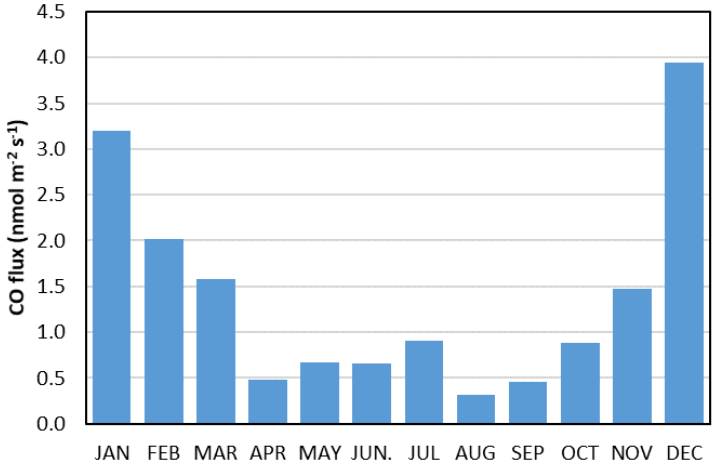

Figure 7: Seasonal variation of the monthly mean carbon monoxide flux from the (quasi)natural grid cells.

3.4 Possible drivers of the ecosystem carbon monoxide budget

To identify the processes controlling the carbon monoxide exchange of ecological systems, we considered footprints in which at least 80% of the measured flux contribution came from within a 5 km radius of the tower and within which the contribution of populated grid cells was no more than 2.5 % (see Section 3.3). The correlation coefficients between UV radiation, photosynthetically active radiation, daytime/nighttime air temperature, soil water content and CO flux, as well as their probability levels, are presented in Fig. 8. The results suggest that solar radiation plays an important role in the CO emission of the soil/vegetation system. The correlation with air temperature at 10 m is not statistically significant at a reasonable probability level for most of the year (standard air temperature measurements or soil temperature data were not available at our site). The nighttime correlations between CO net flux and temperature are not significant either (Fig. 8), suggesting that the summer daytime correlation is the result of the high correlation between the temperature and radiation (Fig. 9).

Soil moisture or soil water content is occasionally also mentioned as one of the drivers of CO exchange (Laasonen et al., 2025). However, here, the correlation between CO flux and local soil water content (SWC) in the top 0-7 cm layer is not statistically significant (Fig. 8). This suggests that SWC may not be an important driver, at least at the given soil/vegetation characteristics.

https://doi.org/10.5194/egusphere-2026-1077
Preprint. Discussion started: 5 May 2026

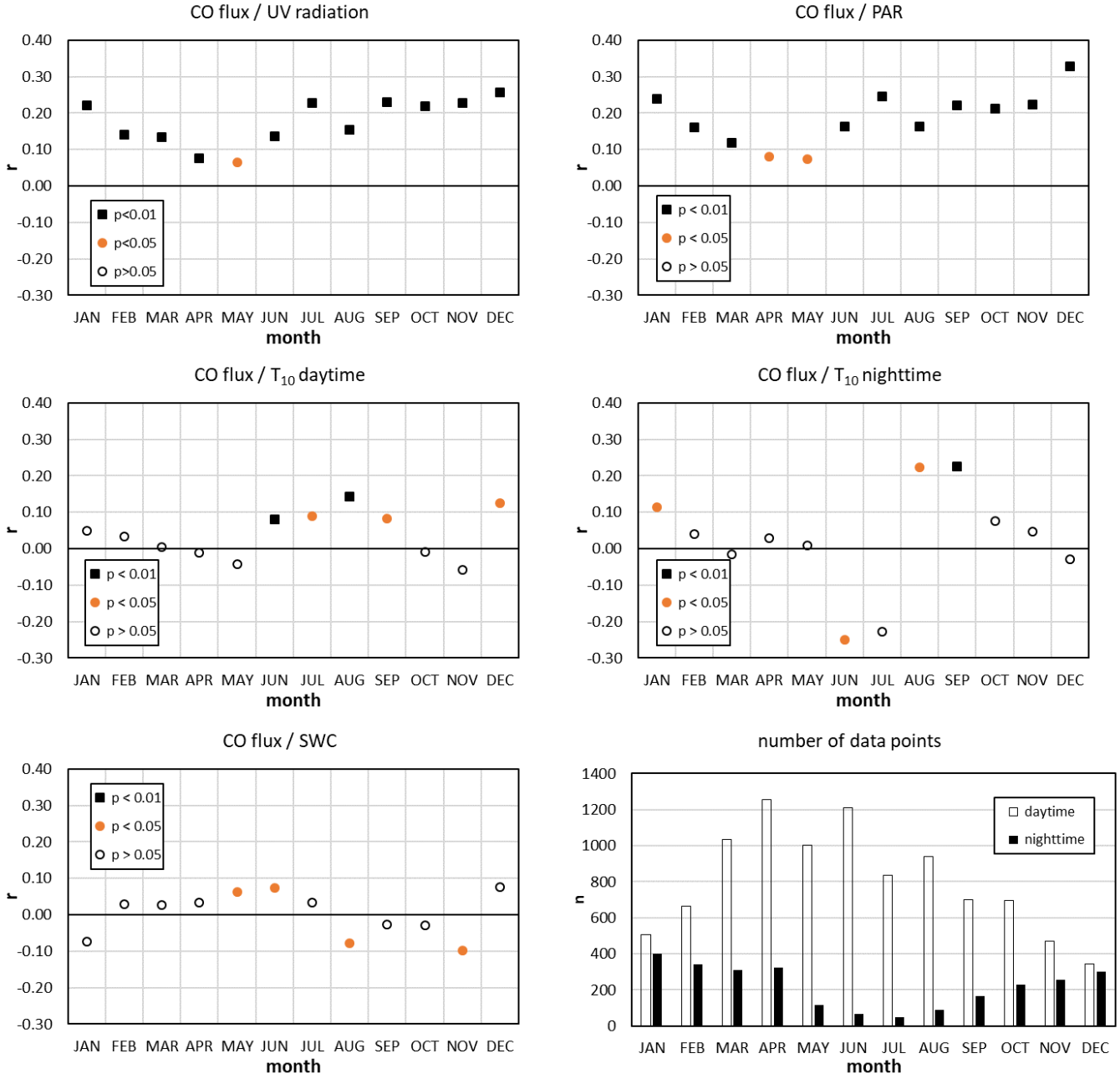

Figure 8: Monthly correlations (2015-2025) of CO fluxes with UV radiation, photosynthetically active radiation (PAR), air temperature at 10 m (T_{10} – day and night), and soil water content, as well as the number of data points available for the correlation calculations. The different symbols indicate the confidence level of the correlation coefficients.

https://doi.org/10.5194/egusphere-2026-1077
Preprint. Discussion started: 5 May 2026

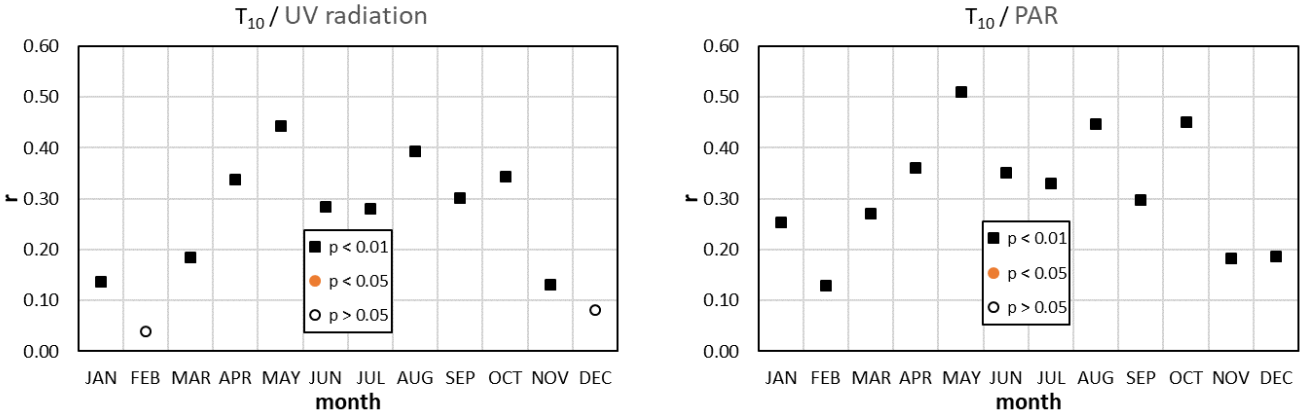

Figure 9: Correlations between air temperature and solar radiation. The wintertime low level of correlation is not a surprise. That time of the year, clear sky usually comes together with cold air mass intrusions.

4 Discussion

4.1 Carbon monoxide emission from the populated areas

The fluxes originating from the populated grid cells show a remarkable seasonal variation: the winter values are an order of magnitude higher than the summer ones (Fig. 5). Since traffic-related emissions may be similar throughout the year, and since there is no notable industrial activity in the region, the additional winter emissions can be reasonably attributed to residential heating in the villages. Although natural gas is available for residential heating, many households in this relatively poor, slowly depopulating region use biomass (wood, agricultural waste) or low-quality coal in technologically outdated, inefficient, poorly ventilated heating appliances. Unfortunately, illegal household waste burning is also rather common in such regions with poor socioeconomic conditions (Haszpra et al., 2022; Balogh et al., 2025). These circumstances can result in high carbon monoxide emissions.

According to the EDGAR v8.1_AP database (European Commission Joint Research Centre and Netherlands Environmental Assessment Agency, 2024) containing 0.1°x0.1° gridded CO emission data up to 2022, approximately 98 % of anthropogenic emissions from the EDGAR grid cell surrounding the monitoring site origined from road transport (IPCC 2006 category: 1.A.3.b (IPCC, 2006)) and residential (IPCC 2006 category: 1.A.4) emissions in 2015–2022. Transport emissions hardly change throughout the year. According to the database, the residential emissions in summer are only about 10 % of the transport emissions. Our measurement recorded 15.2 nmol m^{-2} s^{-1} CO emissions for May-September on average, of which 13.7 nmol m^{-2} s^{-1} may be attributed to the transport sector. The populated grid cells for which this value was calculated cover 12.8 % of the EDGAR grid cell (84.3 km^2) surrounding the tower. Considering the summer value to be valid for the entire year, the total emissions of transport origin are 131 Mg yr^{-1} from the EDGAR grid cell. This value is twice the EDGAR v8.1 average for the years 2015–2022 (60 Mg yr^{-1}).

https://doi.org/10.5194/egusphere-2026-1077
Preprint. Discussion started: 5 May 2026

The total measured anthropogenic emissions are around 460 Mg yr^{-1}, from which 330 Mg yr^{-1} can be attributed to residential activity, primarily heating. Although we neglected small terms in the above estimation, including the few percentage shares of non-transport/non-residential emissions and the anthropogenic emissions recorded in the agricultural/forest areas, the EDGAR data for the residential sector (83 Mg yr^{-1}, averaged for 2015–2022) seems far too low. In addition, we cannot see the reasons for the 30 % reduction in emissions reported by EDGAR for the period from 2015 to 2022. Given the economic stagnation and deterioration between 2015 and 2022, including the impact of the COVID pandemic, we would expect an increase in the burning of biomass and other waste, and thus an increase in carbon monoxide emissions, although this cannot be substantiated in the absence of surveys. Unfortunately, the small share of the populated grid cells in our monitoring area and the resulting limited amount of data prevent us from determining the actual emission trends.

4.2 Carbon monoxide exchange of the vegetation-dominated landscape

The dominant role of photodegradation in natural CO emission and the less intensive solar radiation during the winter months should result in less positive net CO exchange, even if the microbiological CO uptake must also be lower due to the lower temperature. However, the seasonal variation of CO exchange in the agricultural/forested areas shows a maximum in winter (Fig. 7). Murphy et al. (2023) also observed a winter increase in the CO fluxes over a grassland. Despite performing EC measurements on a 2.2-meter-tall tower with a limited footprint, they identified the influence of distant anthropogenic sources. The area influencing our measurements performed at 82 m elevation can be about two orders of magnitude larger, and may cover different distant anthropogenic sources. This is true even when the "clean air" sector is carefully selected and constrained to footprints for which the contribution of the distant sources (outside of the 5 km radius of the tower) to the flux measured at the tower is less than 20 %. The wintertime emission in the populated grid cells can be two to three orders of magnitude larger than in the (quasi)natural grid cells. Even if the weighted footprint contribution from a distant grid cell is minor, the potentially huge emission from that cell may significantly influence the measured fluxes. This effect cannot be completely eliminated with our rather simple correction algorithm.

Not forgetting about the unavoidable seasonally varying anthropogenic influence, our measurements show that agricultural fields and forests are net sources of carbon monoxide throughout the year.

The diurnal variation of the CO exchange in the arable land/forest (i.e. vegetation-covered) sector shows a daytime maximum (Fig. 6), which is more pronounced during the summer half-year. The nighttime net flux tends to be negative, though it does not deviate statistically significantly from zero throughout the year. The average emission for the summer half-year (April–September), when the unavoidable anthropogenic influence is the lowest, is 0.58 nmol m^{-2} s^{-1} based on the monthly averages calculated from the hourly median values. The range is 0.31–0.91 nmol m^{-2} s^{-1}, with the highest value occurring in July. The daily peaks of the median hourly emissions range from 1.59 to 2.66 nmol m^{-2} s^{-1}. The nighttime (20-04 h LST) hourly median values range from -1.01 to +1.17 nmol m^{-2} s^{-1}, respectively. These values fall within the range of other measurements of -3 – +14 nmol m^{-2} s^{-1} over grasslands and arable lands (van Asperen et al., 2015; Pihlatie et al., 2016; Cowan et al., 2018).

https://doi.org/10.5194/egusphere-2026-1077
Preprint. Discussion started: 5 May 2026

The longer-term EC measurements recorded diurnal CO flux variations similar to our measurements. Pihlatie et al. (2016) reported a distinct diurnal pattern with uptake at night and emission during the day, with maximum emissions at noon. The daytime maximum median emissions over the perennial reed canary grass field monitored reached 2.7 nmol m^{-2} s^{-1} around noon, while the nighttime values varied around -0.77 nmol m^{-2} s^{-1} throughout the measurement period. Cowan et al. (2018) also measured fluxes that showed a regular diurnal cycle peaking at noon (1–4 nmol m^{-2} s^{-1}) and falling to around zero (>-1 nmol m^{-2} s^{-1}) at night. Laasonen (2021) recorded daytime net emission up to 3 nmol m^{-2} s^{-1} in forest, wetland, and cropland ecosystems in summer. These ecosystems showed zero flux or small uptake during nighttime. Murphy et al. (2023) observed a similar diurnal pattern, also in summer. During daytime, the measured fluxes were 1–5 nmol m^{-2} s^{-1}, while the nighttime values were near zero or slightly negative (>-2 nmol m^{-2} s^{-1}). Recent measurements of Laasonen et al. (2025) over peatland also showed the characteristic daily cycle with a daytime maximum of 1.1 nmol m^{-2} s^{-1} and a nighttime minimum of -0.44 nmol m^{-2} s^{-1}.

EC measurements at an elevation of 82 m would require the calculation of the storage term, i.e., the amount of carbon monoxide accumulating below the measurement elevation in the cases of decoupling from the surface due to low-level temperature inversions (Haszpra et al., 2005). Ignoring the storage term can result in unrealistic flux values when the inversion layer breaks up. Due to the lack of concentration profile measurements, we could not calculate the storage term. However, the lack of a negative or positive peak in the fluxes measured during the break-up of the inversion layer indicates that no significant accumulation or depletion occurs in the surface layer, and the net emission at the surface at night is close to zero indeed.

4.3 Drivers of the ecosystem carbon monoxide budget

Scientific publications widely complain that we know very little about the soil and vegetation processes that can produce or absorb carbon monoxide (King, 2000; Constant et al., 2008; Bruhn et al., 2013; Liu et al., 2018; Sun et al., 2018; Laasonen et al., 2025). This also hinders the development of process-based biogeochemistry CO exchange models (Liu et al., 2018). From the atmospheric point of view, the commonly studied drivers are solar radiation (see e.g. Bruhn et al., 2013; van Asperen et al., 2015; Pihlatie et al., 2016; Cowan et al., 2018; Murphy et al., 2023; Laasonen et al., 2025; and references therein), temperature (Constant et al., 2008; van Asperen et al., 2015; Murphy et al., 2023; van Asperen et al., 2024), and soil moisture (Cowan et al., 2018; Murphy et al., 2023; Laasonen et al., 2025). However, the results are uncertain and partly controversial, presumably due to the different climate and soil conditions, different vegetation types at the measurement sites, as well as the short measurement durations.

Most previous studies agree that photo and/or thermal degradation of organic substances is/are the main driver(s) of the ecosystems' CO emissions. The role of solar radiation (global radiation, UV or PAR spectra of the visible range) in CO emission has been well-established since the early studies on natural CO flux (see e.g. Seiler and Giehl, 1977; Tarr et al., 1995; Schade et al., 1999; Bruhn et al., 2013; Pihlatie et al., 2016; Murphy et al., 2023; Laasonen et al., 2025; and references therein). However, the importance of the role of thermal degradation is somewhat controversial. One of the reasons is that

https://doi.org/10.5194/egusphere-2026-1077
Preprint. Discussion started: 5 May 2026

both emissions resulting from the abiotic thermal degradation and microbiological uptake are temperature dependent (Whalen and Reeburgh, 2001). Some of the methods applied in the field (e.g. micrometeorological methods) measure the net surface-atmosphere exchange and cannot separate the emission and uptake processes. On the other hand, temperature is strongly correlated with solar insolation. According to the measurements of Laasonen et al. (2025), solar radiation is the primary driver of CO flux; the role of the air temperature is limited. Murphy et al. (2023) and Cowan et al. (2018) found a variable relation between CO flux and temperature. On the contrary, the laboratory and field measurements of van Asperen et al. (2015) indicated the higher importance of thermal degradation in CO flux relative to photo degradation.

Our measurements support the assumption that thermal decomposition either plays a minor role in CO emissions or is largely compensated by the microbiological uptake. The collinearity between temperature and radiation can lead to the incorrect identification of the causal relationships that may explain the controversy in the literature.

The role of SWC as a driver cannot be confirmed by our results. However, it should be noted that SWC may vary greatly within the footprint area due to the diversity of land use (presence of summer and winter crops with different phenophases, associated rooting depths, evapotranspiration rates, etc.). Therefore, the above conclusion should be treated with caution.

5 Conclusions

The evaluation of the 10-year-long tall tower EC-based carbon monoxide flux measurements has revealed the advantages and challenges of such monitoring projects. The tall-tower EC measurements and their associated large flux footprints can provide information on heterogeneous, regionally characteristic landscapes that help the upscaling of the results. However, the high elevation and the occasional decoupling from the surface cause gaps in the data series. In principle, footprint modelling can separate the flux contribution from different land cover types. However, the emissions from populated areas are magnitudes larger than the carbon monoxide (CO) exchange of natural or quasi-natural (agricultural fields, grasslands, forests) areas. Therefore, even distant anthropogenic sources can significantly influence measurements with footprints in areas covered almost exclusively by vegetation. This makes it difficult to study the dynamics of the CO exchange of the soil-vegetation system.

Despite the above-mentioned difficulties, our measurements support the theory that the primary driver of the CO exchange of the (quasi)natural ecosystems is solar radiation. The maximum emission can be observed in summer daytime (up to 2.66 nmol m^{-2} s^{-1}, July hourly median at noon), while the nighttime exchange does not deviate statistically significantly from zero.

The measured emissions from the populated areas significantly exceed the emissions calculated using activity statistics. The factors of 2–4 are far too large to be attributable to the uncertainty in the methodology and the uncertainty of the input data, but certainly reflect the underestimation of the real-world emission factors. It is hypothesized that the bottom-up method underestimates the fact that in this natural gas-supplied region, a significant proportion of the population heats their homes with technologically outdated heating appliances using wood, low-quality coal, or agricultural waste for economic reasons, in some cases also burning household waste. Atmospheric effects depend on the amount of carbon monoxide actually

https://doi.org/10.5194/egusphere-2026-1077
Preprint. Discussion started: 5 May 2026

released into the air, so it would be necessary to refine the emission factors applicable in real-life situations through field measurements. If the anthropogenic emission density recorded in the region of our measurement site were representative of the other rural regions in the country, the national total emissions reported to international organizations would need to be modified upward.

Data availability

The data used in the study are available at https://doi.org/10.5281/zenodo.20025124.

Author contributions

L.H. designed the study, performed the calculations, and wrote the original manuscript; Z.B. performed the eddy covariance calculations; A.K. provided the land use information and visualization; N.K. supported the footprint calculations. All authors read and edited the original manuscript.

Competing interests

The authors declare that they have no competing financial interests or personal relationships that could have appeared to influence the work reported in this paper.

Acknowledgements

This work has been partly implemented by the National Multidisciplinary Laboratory for Climate Change (RRF-2.3.1-21-2022-00014) project within the framework of Hungary's National Recovery and Resilience Plan supported by the Recovery and Resilience Facility of the European Union. Also supported by the “Advanced methods of greenhouse gases emission reduction and sequestration in agriculture and forest landscape for climate change mitigation” (CZ.02.01.01/00/22_008/0004635) project, and the French-Hungarian bilateral partnership through the BALATON (N° 44703TF)/TéT (2019-2.1.11-TÉT-2019-00031) programme. The research has been supported by the Hungarian National Scientific Research Fund (NKFIH FK-146600). The N_2O/CO/H_2O measurements used in this study are also used in and partially supported by the European Union Horizon Europe PARIS project (Process Attribution of Regional Emissions – Grant Agreement no. 101081430). The research presented in this paper is also a contribution to the Strategic Research Area “ModElling the Regional and Global Earth system”, MERGE, funded by the Swedish government. The measurement site was provided by Antenna Hungária Corporation.

https://doi.org/10.5194/egusphere-2026-1077
Preprint. Discussion started: 5 May 2026

Besides the author's statement of gratitude to and recognition of the people and institutions that helped the author's research and writing, authors are also asked to include relevant research infrastructure they have benefitted from during their research, where research was conducted or data/resources were used. Examples are Field Stations and Marine Laboratories (FSMLs).

References

Aubinet, M., Vesala, T., Papale, D., and (eds.): Eddy covariance: A practical guide to measurement and data analysis, Springer, Dordrecht - Heidelberg - London - New York, https://doi.org/10.1007/978-94-007-2351-1, 2012.

Balogh, B. S., Csákó, Z., Nyiri, Z., Berlinger, B., Molnár, M., Major, I., Gergely, V., and Szigeti, T.: Residential solid fuel combustion and its contribution to air pollution in Hungary: A comparative study, Atmospheric Environment, 360, 121399, https://doi.org/10.1016/j.atmosenv.2025.121399, 2025.

Barcza, Z.: Long term atmosphere/biosphere exchange of CO_2 in Hungary, Ph.D. Thesis, Eötvös Loránd University, Department of Meteorology, Budapest. (Supervisor: T. Weidinger, scientific adviser: L. Haszpra), http://nimbus.elte.hu/~bzoli/thesis/, 2001.

Barcza, Z., Kern, A., Davis, K. J., and Haszpra, L.: Analysis of the 21-years long carbon dioxide flux dataset from a Central European tall tower site, Agricultural and Forest Meteorology, 290, 108027, https://doi.org/10.1016/j.agrformet.2020.108027, 2020.

Barcza, Z., Kern, A., Haszpra, L., and Kljun, N.: Spatial representativeness of tall tower eddy covariance measurements using remote sensing and footprint analysis, Agricultural and Forest Meteorology, 149, 795-807, https://doi.org/10.1016/j.agrformet.2008.10.021, 2009.

Berger, B. W., Davis, K. J., Yi, C., Bakwin, P. S., and Zhao, C. L.: Long-term carbon dioxide fluxes from a very tall tower in a northern forest: Flux measurement methodology, Journal of Atmospheric and Oceanic Technology, 18, 529-542, https://doi.org/10.1175/1520-0426(2001)018<0529:LTCDFF>2.0.CO;2, 2001.

Blomquist, B. W., Fairall, C. W., Huebert, B. J., and Wilson, S. T.: Direct measurement of the oceanic carbon monoxide flux by eddy correlation, Atmos. Meas. Tech., 5, 3069-3075, https://doi.org/10.5194/amt-5-3069-2012, 2012.

Bruhn, D., Albert, K. R., Mikkelsen, T. N., and Ambus, P.: UV-induced carbon monoxide emission from living vegetation, Biogeosciences, 10, 7877-7882, https://doi.org/10.5194/bg-10-7877-2013, 2013.

Chi, J., Nilsson, M. B., Kljun, N., Wallerman, J., Fransson, J. E. S., Laudon, H., Lundmark, T., and Peichl, M.: The carbon balance of a managed boreal landscape measured from a tall tower in northern Sweden, Agricultural and Forest Meteorology, 274, 29-41, https://doi.org/10.1016/j.agrformet.2019.04.010, 2019.

Constant, P., Poissant, L., and Villemur, R.: Annual hydrogen, carbon monoxide and carbon dioxide concentrations and surface to air exchanges in a rural area (Québec, Canada). Atmospheric Environment, 42, 5090-5100., https://doi.org/10.1016/j.atmosenv.2008.02.021, 2008.

https://doi.org/10.5194/egusphere-2026-1077
Preprint. Discussion started: 5 May 2026

Copernicus Climate Change Service: ERA5-Land hourly data from 1950 to present, Copernicus Climate Change Service Climate Data Store, - accessed 15 September 2025, https://doi.org/10.24381/cds.e2161bac, 2022.

Cowan, N., Helfter, C., Langford, B., Coyle, M., Levy, P., Moxley, J., Simmons, I., Leeson, S., Nemitz, E., and Skiba, U.: Seasonal fluxes of carbon monoxide from an intensively grazed grassland in Scotland, Atmospheric Environment, 194, 170-178, https://doi.org/10.1016/j.atmosenv.2018.09.039, 2018.

Coimbra, P. H., Loubet, B., Laurent, O., Bignotti, L., Lozano, M., and Ramonet, M.: Eddy covariance with slow-response greenhouse gas analysers on tall towers: bridging atmospheric and ecosystem greenhouse gas networks, Atmos. Meas. Tech., 17, 6625-6645, https://doi.org/10.5194/amt-17-6625-2024, 2024.

Crutzen, P. J., Lawrence, M. G., and Pöschl, U.: On the background photochemistry of tropospheric ozone, Tellus B: Chemical and Physical Meteorology, https://doi.org/10.3402/tellusb.v51i1.16264, 1999.

Davis, K. J., Bakwin, P. S., Yi, C., Berger, B. W., Zhao, C., Teclaw, R. M., and Isebrands, J. G.: The annual cycles of CO_2 and H_2O exchange over a northern mixed forest as observed from a very tall tower, Global Change Biology, 9, 1278–1293, https://doi.org/10.1046/j.1365-2486.2003.00672.x, 2003.

Desai, A. R., Xu, K., Tian, H., Weishampel, P., Thom, J., Baumann, D., Andrews, A. E., Cook, B. D., King, J. Y., and Kolka, R.: Landscape-level terrestrial methane flux observed from a very tall tower, Agricultural and Forest Meteorology, 201, 61-75, https://doi.org/10.1016/j.agrformet.2014.10.017, 2015.

Duncan, B. N., Logan, J. A., Bey, I., Megretskaia, I. A., Yantosca, R. M., Novelli, P. C., Jones, N. B., and Rinsland, C. P.: Global budget of CO, 1988-1997: Source estimates and validation with a global model, J. of Geophysical Research, 112D, D22301, https://doi.org/10.1029/2007JD008459, 2007.

European Commission, Joint Research Centre. and Netherlands Environmental Assessment Agency: Emission Database for Global Atmospheric Research (EDGAR), release version 8.1_AP 1970-2022, https://edgar.jrc.ec.europa.eu/dataset_ap81, last visited on 21 October 2025, 2024.

Gaubert, B., Worden, H. M., Arellano, A. F. J., Emmons, L. K., Tilmes, S., Barré, J., Martinez Alonso, S., Vitt, F., Anderson, J. L., Alkemade, F., Houweling, S., and Edwards, D. P.: Chemical feedback from decreasing carbon monoxide emissions, Geophysical Research Letters, 44, 9985-9995, https://doi.org/10.1002/2017gl074987, 2017.

Haszpra, L. and Barcza, Z.: Climate variability as reflected in a regional atmospheric CO_2 record, Tellus, 62B, 417-426, https://doi.org/10.1111/j.1600-0889.2010.00505.x, 2010.

Haszpra, L., Barcza, Z., Davis, K. J., and Tarczay, K.: Long term tall tower carbon dioxide flux monitoring over an area of mixed vegetation, Agricultural and Forest Meteorology, 132, 58-77, https://doi.org/10.1016/j.agrformet.2005.07.002, 2005.

Haszpra, L., Barcza, Z., Bakwin, P. S., Berger, B. W., Davis, K. J., and Weidinger, T.: Measuring system for the long-term monitoring of biosphere/atmosphere exchange of carbon dioxide, J. of Geophysical Research, 106D, 3057-3070, https://doi.org/10.1029/2000JD900600, 2001.

https://doi.org/10.5194/egusphere-2026-1077
Preprint. Discussion started: 5 May 2026

Haszpra, L., Barcza, Z., Ferenczi, Z., Hollós, R., Kern, A., and Kljun, N.: Real-world wintertime CO, N_2O, and CO_2 emissions of a central European village, Atmos. Meas. Tech., 15, 5019-5031, https://doi.org/10.5194/amt-15-5019-2022, 2022.

Hedelius, J. K., Toon, G. C., Buchholz, R. R., Iraci, L. T., Podolske, J. R., Roehl, C. M., Wennberg, P. O., Worden, H. M., and Wunch, D.: Regional and urban column CO trends and anomalies as observed by MOPITT over 16 years, Journal of Geophysical Research: Atmospheres, 126, e2020JD033967, https://doi.org/10.1029/2020JD033967, 2021.

Heidbach, K., Schmid, H. P., and Mauder, M.: Experimental evaluation of flux footprint models, Agricultural and Forest Meteorology, 246, 142-153, https://doi.org/10.1016/j.agrformet.2017.06.008, 2017.

Helbig, M., Chasmer, L. E., Kljun, N., Quinton, W. L., Treat, C. C., and Sonnentag, O.: The positive net radiative greenhouse gas forcing of increasing methane emissions from a thawing boreal forest-wetland landscape, Global Change Biology, 23, 2413-2427, https://doi.org/https://doi.org/10.1111/gcb.13520, 2017.

Helfter, C., Tremper, A. H., Halios, C. H., Kotthaus, S., Bjorkegren, A., Grimmond, C. S. B., Barlow, J. F., and Nemitz, E.: Spatial and temporal variability of urban fluxes of methane, carbon monoxide and carbon dioxide above London, UK, Atmos. Chem. Phys., 16, 10543-10557, 10.5194/acp-16-10543-2016, 2016.

Hernandez Rodriguez, L. C., Goodwell, A. E., and Kumar, P.: Inside the flux footprint: The role of organized land cover heterogeneity on the dynamics of observed land-atmosphere exchange fluxes, Frontiers in Water, Volume 5 - 2023, https://doi.org/10.3389/frwa.2023.1033973, 2023.

Hilland, R., Hashemi, J., Stagakis, S., Brunner, D., Constantin, L., Kljun, N., Kunz, A. K., Molinier, B., Hammer, S., Emmenegger, L., and Christen, A.: Sectoral attribution of greenhouse gas and pollutant emissions using multi-species eddy covariance on a tall tower in Zurich, Switzerland, Atmos. Chem. Phys., 25, 14279-14299, https://doi.org/10.5194/acp-25-14279-2025, 2025.

Holtslag, A. A. M. and Nieuwstadt, F. T. M.: Scaling the atmospheric boundary layer, Boundary-Layer Meteorology, 36, 201-209, https://doi.org/10.1007/bf00117468, 1986.

Horner, J. M.: Anthropogenic emissions of carbon monoxide, Reviews on Environmental Health, 15, 289-298, https://doi.org/10.1515/REVEH.2000.15.3.289, 2000.

Hungarian Central Statistical Office: Hegyhátsál, Detailed Gazeteer, https://www.ksh.hu/apps/hntr.telepules?p_lang=EN&p_id=30216, - last accessed 19 September 2025, 2025.

IPCC: 2006 IPCC Guidelines for National Greenhouse Gas Inventories - Prepared by the National Greenhouse Gas Inventories Programme (Eds.: Eggleston H.S., Buendia L., Miwa K., Ngara T. and Tanabe K.) https://www.ipcc-nggip.iges.or.jp/public/2006gl/, 2006.

Khalil, M. A. K., Pinto, J. P., and Shearer, M. J.: Atmospheric carbon monoxide, Chemosphere - Global Change Science, 1, ix-xi, https://doi.org/10.1016/S1465-9972(99)00053-7, 1999.

King, G., M.: Land use impacts on atmospheric carbon monoxide consumption by soils, Global Biogeochem. Cycles, 14, 1161-1172, https://doi.org/10.1029/2000GB001272, 2000.

https://doi.org/10.5194/egusphere-2026-1077
Preprint. Discussion started: 5 May 2026

King, G. M. and Weber, C. F.: Distribution, diversity and ecology of aerobic CO-oxidizing bacteria, Nature Reviews Microbiology, 5, 107-118, https://doi.org/10.1038/nrmicro1595, 2007.

Kljun, N., Rotach, M. W., and Schmid, H. P.: A three-dimensional backward Lagrangian footprint model for a wide range of boundary-layer stratifications, Boundary-Layer Meteorology, 103, 205-226, https://doi.org/10.1023/A:1014556300021, 2002.

Kljun, N., Calanca, P., Rotach, M. W., and Schmid, H. P.: A Simple Parameterisation for Flux Footprint Predictions, Boundary-Layer Meteorology, 112, 503-523., https://doi.org/10.1023/B:BOUN.0000030653.71031.96, 2004.

Kljun, N., Calanca, P., Rotach, M. W., and Schmid, H. P.: A simple two-dimensional parameterisation for Flux Footprint Prediction (FFP), Geosci. Model Dev., 8, 3695-3713, https://doi.org/10.5194/gmd-8-3695-2015, 2015.

Laasonen, A.: Biogenic carbon monoxide fluxes in four terrestrial ecocystems, MS thesis, University of Helsinki, Faculty of Science, http://hdl.handle.net/10138/337751, 2021.

Laasonen, A., Buzacott, A., Kohonen, K. M., Lundin, E., Meire, A., Pihlatie, M., and Mammarella, I.: Radiation and surface wetness drive carbon monoxide fluxes from an Arctic peatland, Biogeosciences, 22, 7505-7518, https://doi.org/10.5194/bg-22-7505-2025, 2025.

Lee, X.: On micrometeorological observations of surface-air exchange over tall vegetation, Agricultural and Forest Meteorology, 91, 39-49, https://doi.org/10.1016/S0168-1923(98)00071-9, 1998.

Lelieveld, J., Gromov, S., Pozzer, A., and Taraborrelli, D.: Global tropospheric hydroxyl distribution, budget and reactivity, Atmos. Chem. Phys., 16, 12477-12493, https://doi.org/10.5194/acp-16-12477-2016, 2016.

Liu, L., Zhuang, Q., Zhu, Q., Liu, S., van Asperen, H., and Pihlatie, M.: Global soil consumption of atmospheric carbon monoxide: an analysis using a process-based biogeochemistry model, Atmos. Chem. Phys., 18, 7913-7931, https://doi.org/10.5194/acp-18-7913-2018, 2018.

Magyar Közút: Az országos közutak 2023. évre vonatkozó keresztmetszeti forgalma https://internet.kozut.hu/download/az-orszagos-kozutak-2023-evre-vonatkozo-keresztmetszeti-forgalma/, - last accessed 19 September 2025, 2025.

Massman, W. J.: The attenuation of concentration fluctuations in turbulent flow through a tube, Journal of Geophysical Research: Atmospheres, 96, 15269-15273, https://doi.org/10.1029/91jd01514, 1991.

Moore, C. J.: Frequency response corrections for eddy correlation systems, Boundary-Layer Meteorology, 37, 17-35, https://doi.org/10.1007/bf00122754, 1986.

Murphy, R. M., Lanigan, G., Martin, D., and Cowan, N.: Carbon monoxide fluxes measured using the eddy covariance method from an intensively managed grassland in Ireland, Environmental Science: Atmospheres, 3, 1834-1846, https://doi.org/10.1039/d3ea00112a, 2023.

Peltola, O., Hensen, A., Belelli Marchesini, L., Helfter, C., Bosveld, F. C., van den Bulk, W. C. M., Haapanala, S., van Huissteden, J., Laurila, T., Lindroth, A., Nemitz, E., Röckmann, T., Vermeulen, A. T., and Mammarella, I.: Studying the spatial variability of methane flux with five eddy covariance towers of varying height, Agricultural and Forest Meteorology, 214–215, 456-472, https://doi.org/10.1016/j.agrformet.2015.09.007, 2015.

https://doi.org/10.5194/egusphere-2026-1077
Preprint. Discussion started: 5 May 2026

Pihlatie, M., Rannik, Ü., Haapanala, S., Peltola, O., Shurpali, N., Martikainen, P. J., Lind, S., Hyvönen, N., Virkajärvi, P., Zahniser, M., and Mammarella, I.: Seasonal and diurnal variation in CO fluxes from an agricultural bioenergy crop, Biogeosciences, 13, 5471-5485, https://doi.org/10.5194/bg-13-5471-2016, 2016.

Ragsdale, S. W.: Life with carbon monoxide, Critical Reviews in Biochemistry and Molecular Biology, 39, 165-195, https://doi.org/10.1080/10409230490496577, 2004.

Rey-Sanchez, C., Arias-Ortiz, A., Kasak, K., Chu, H., Szutu, D., Verfaillie, J., and Baldocchi, D.: Detecting hot spots of methane flux using footprint-weighted flux maps, Journal of Geophysical Research: Biogeosciences, 127, e2022JG006977, https://doi.org/10.1029/2022JG006977, 2022.

Schade, G. W., Hofmann, R.-M., and Crutzen, P. J.: CO emissions from degrading plant matter (I): Measurements, Tellus B: Chemical and Physical Meteorology, 51, 889-908, https://doi.org/10.3402/tellusb.v51i5.16501, 1999.

Schmidt, G. A., Ruedy, R. A., Miller, R. L., and Lacis, A. A.: Attribution of the present-day total greenhouse effect., J. of Geophysical Research, 115D, D20106, https://doi.org/10.1029/2010JD014287, 2010.

Seiler, W. and Giehl, H.: Influence of plants on the atmospheric carbon monoxide, Geophysical Research Letters, 4, 329-332, https://doi.org/10.1029/GL004i008p00329, 1977.

Sun, W., Kooijmans, L. M. J., Maseyk, K., Chen, H., Mammarella, I., Vesala, T., Levula, J., Keskinen, H., and Seibt, U.: Soil fluxes of carbonyl sulfide (COS), carbon monoxide, and carbon dioxide in a boreal forest in southern Finland, Atmos. Chem. Phys., 18, 1363-1378, https://doi.org/10.5194/acp-18-1363-2018, 2018.

Szopa, S., Naik, V., Adhikary, B., Artaxo, P., Berntsen, T., Collins, W. D., Fuzzi, S., Gallardo, L., Kiendler-Scharr, A., Z. Klimont, Liao, H., Unger, N., and Zani, P.: Short-lived Climate Forcers, In Climate Change 2021: The Physical Science Basis. Contribution of Working Group I to the Sixth Assessment Report of the Intergovernmental Panel on Climate Change [Masson-Delmotte, V., P. Zhai, A. Pirani, S.L. Connors, C. Péan, S. Berger, N. Caud, Y. Chen, L. Goldfarb, M.I. Gomis, M. Huang, K. Leitzell, E. Lonnoy, J.B.R. Matthews, T.K. Maycock, T. Waterfield, O. Yelekçi, R. Yu, and B. Zhou (eds.)]. Cambridge University Press, Cambridge, United Kingdom and New York, NY, USA, 817-922, https://doi.org/10.1017/9781009157896.008, 2023.

Tanács, E., Belényesi, M., Lehoczki, R., Pataki, R., Petrik, O., Standovár, T., Pásztor, L., Laborczi, A., Szatmári, G., Molnár, Z., Bede-Fazekas, Á., Somodi, I., Kristóf, D., Kovács-Hostyánszki, A., Török, K., Kisné Fodor, L., Zsembery, Z., Friedl, Z., and Maucha, G.: Compiling a high-resolution country-level ecosystem map to support environmental policy: methodological challenges and solutions from Hungary, Geocarto International, 37, 8746-8769, https://doi.org/10.1080/10106049.2021.2005158, 2021.

Tarr, M. A., Miller, W. L., and Zepp, R. G.: Direct carbon monoxide photoproduction from plant matter, Journal of Geophysical Research: Atmospheres, 100, 11403-11413, https://doi.org/10.1029/94JD03324, 1995.

Tikkasalo, O. P., Peltola, O., Alekseychik, P., Heikkinen, J., Launiainen, S., Lehtonen, A., Li, Q., Martínez-García, E., Peltoniemi, M., Salovaara, P., Tuominen, V., and Mäkipää, R.: Eddy-covariance fluxes of CO_2, CH_4 and N_2O in a drained peatland forest after clear-cutting, Biogeosciences, 22, 1277-1300, https://doi.org/10.5194/bg-22-1277-2025, 2025.

https://doi.org/10.5194/egusphere-2026-1077
Preprint. Discussion started: 5 May 2026

Tuovinen, J. P., Aurela, M., Hatakka, J., Räsänen, A., Virtanen, T., Mikola, J., Ivakhov, V., Kondratyev, V., and Laurila, T.: Interpreting eddy covariance data from heterogeneous Siberian tundra: land-cover-specific methane fluxes and spatial representativeness, Biogeosciences, 16, 255-274, https://doi.org/10.5194/bg-16-255-2019, 2019.

van Asperen, H., Warneke, T., Sabbatini, S., Nicolini, G., Papale, D., and Notholt, J.: The role of photo- and thermal degradation for CO_2 and CO fluxes in an arid ecosystem, Biogeosciences, 12, 4161-4174, https://doi.org/10.5194/bg-12-4161-2015, 2015.

van Asperen, H., Warneke, T., Carioca de Araújo, A., Forsberg, B., José Filgueiras Ferreira, S., Röckmann, T., van der Veen, C., Bulthuis, S., Ramos de Oliveira, L., de Lima Xavier, T., da Mata, J., de Oliveira Sá, M., Ricardo Teixeira, P., Andrews de França e Silva, J., Trumbore, S., and Notholt, J.: The emission of CO from tropical rainforest soils, Biogeosciences, 21, 3183-3199, https://doi.org/10.5194/bg-21-3183-2024, 2024.

van der Molen, M. K., Gash, J. H. C., and Elbers, J. A.: Sonic anemometer (co)sine response and flux measurement: II. The effect of introducing an angle of attack dependent calibration., Agricultural and Forest Meteorology, 122, 95-109., 2004.

Webb, E. K., Pearman, G. I., and Leuning, R.: Correction of flux measurements for density effects due to heat and water vapour transfer, Quarterly Journal of the Royal Meteorological Society, 106, 85-100, https://doi.org/10.1002/qj.49710644707, 1980.

Whalen, S. C. and Reeburgh, W. S.: Carbon monoxide consumption in upland boreal forest soils, Soil Biology and Biochemistry, 33, 1329-1338, https://doi.org/10.1016/S0038-0717(01)00038-4, 2001.

WMO: Twenty-First WMO/IAEA Meeting on Carbon Dioxide, Other Greenhouse Gases and Related Tracers Measurement Techniques (GGMT-2022) (Eds.: A. Crotwell, L. Huang, P. Sperlich, F. Vogel), WMO GAW Report no., 292, https://doi.org/https://library.wmo.int/idurl/4/68925, 2024.

Zhao, Y., Saunois, M., Bousquet, P., Lin, X., Berchet, A., Hegglin, M. I., Canadell, J. G., Jackson, R. B., Deushi, M., Jöckel, P., Kinnison, D., Kirner, O., Strode, S., Tilmes, S., Dlugokencky, E. J., and Zheng, B.: On the role of trend and variability in the hydroxyl radical (OH) in the global methane budget, Atmos. Chem. Phys., 20, 13011-13022, https://doi.org/10.5194/acp-20-13011-2020, 2020.

Zheng, B., Chevallier, F., Yin, Y., Ciais, P., Fortems-Cheiney, A., Deeter, M. N., Parker, R. J., Wang, Y., Worden, H. M., and Zhao, Y.: Global atmospheric carbon monoxide budget 2000–2017 inferred from multi-species atmospheric inversions, Earth Syst. Sci. Data, 11, 1411-1436, https://doi.org/10.5194/essd-11-1411-2019, 2019.